Lab on a Chip

PAPER

View Article Online
View Journal | View Issue

Cite this: *Lab Chip*, 2019, **19**, 3481

Microfluidic quantification and separation of yeast based on surface adhesion†

Kristina Reinmets, [a] Amin Dehkharghani,[b] Jeffrey S. Guasto [b] and Stephen M. Fuchs *[a]

Received 22nd March 2019,
Accepted 26th August 2019

DOI: 10.1039/c9lc00275h

rsc.li/loc

Fungal adhesion is fundamental to processes ranging from infections to food production to bioengineering. Yet, robust, population-scale quantification methods for yeast surface adhesion are lacking. We developed a microfluidic assay to discriminate and separate genetically-related yeast strains based on adhesion strength, and to quantify effects of ionic strength and substrate hydrophobicity on adhesion. This approach will enable the rapid screening and fractionation of yeast based on adhesive properties for genetic protein engineering, anti-fouling surfaces, and a host of other applications.

1. Introduction

Yeast are single-celled eukaryotes that possess the ability to adhere to a range of biotic and abiotic surfaces.[1] Adhesion contributes to pathogenicity in clinical yeast such as *Candida albicans* and *Candida glabrata*,[2] but also imparts desirable qualities to industrial yeast such as *Saccharomyces cerevisiae*.[3] Quantifying the properties of yeast adhesion, as well as environmental factors that mediate interactions between cells and surfaces, is therefore crucial to understanding a host of environmental, medical, and industrial processes. Fungal adhesion is mediated by surface proteins known as adhesins (Fig. 1a), which participate either in the interaction with sugar molecules and proteins on the surface of other yeasts and mammalian cells, or nonspecific binding to abiotic surfaces.[1,4–7]

While yeast adhesin genes exhibit broad genetic diversity, they also show significant structural similarities across related species, including both non-infectious and pathogenic yeast.[8,9] Adhesion of yeast cells to surfaces is an important early step in biofilm formation, which provides an ecological advantage to yeast through nutrient availability and protection from environmental hazards, such as fluid flow, changes in pH, or the presence of toxic antifungal agents. For example, surface attached *C. albicans*, adhered to an abiotic dental prosthetic, were shown to be significantly more resistant to a range of antifungals than the same cells grown planktonically.[10] Likewise, *S. cerevisiae* exhibit the ability to adhere to one another (flocculation), which is important for protection from environmental stresses.[11] Adhesion is also an attribute for certain industrial purposes from beer and wine production to chemical synthesis.[12,13] The availability of vast molecular tools and the robustness of *S. cerevisiae* have made budding yeast an ideal model system for studying the mechanisms of fungal adhesion as well as for exploiting their well-known genetics for bioengineering purposes. However, as surface adhesion may either impede or promote various applications, robust and rapid screening methods for adhesion phenotypes are needed in order to improve our understanding of fungal adhesion.

Previous studies of yeast adhesion have primarily focused on either multicellular cell–cell and cell–surface interactions within biofilms or precision measurements of the adhesive properties of single yeast cells and adhesin proteins.[14] Fungal biofilms encompass complex cellular structures composed of extracellular matrix (ECM) containing polysaccharides and proteins, including fungal adhesins that are shed from cell surface, as well as yeast cells in various differentiation and life stages.[15,16] Standard approaches for studying yeast biofilm adhesion include long term culturing of yeast on agar plates or in liquid media using polystyrene plates, and analysis of biofilm release from the surfaces upon the topical application of a water stream.[17] Adhesion or agar invasion is also approximated using colorimetric cell-staining dyes to stain cells adhered to a surface.[18] Biofilm investigations have greatly contributed to our understanding of complex interactions among cells within the biofilm as well as environmental and biological signals regulating the formation of fungal mats.[19] However, unravelling the fundamental mechanisms of surface attachment of single cells from a complex biofilm community of cells embedded in ECM is challenging. Single-cell studies have helped to illuminate the nanoscale

[a] *Department of Biology, Tufts University, Medford, MA 02155, USA. E-mail: Stephen.fuchs@tufts.edu*
[b] *Department of Mechanical Engineering, Tufts University, MA 02155, USA*
† Electronic supplementary information (ESI) available. See DOI: 10.1039/c9lc00275h

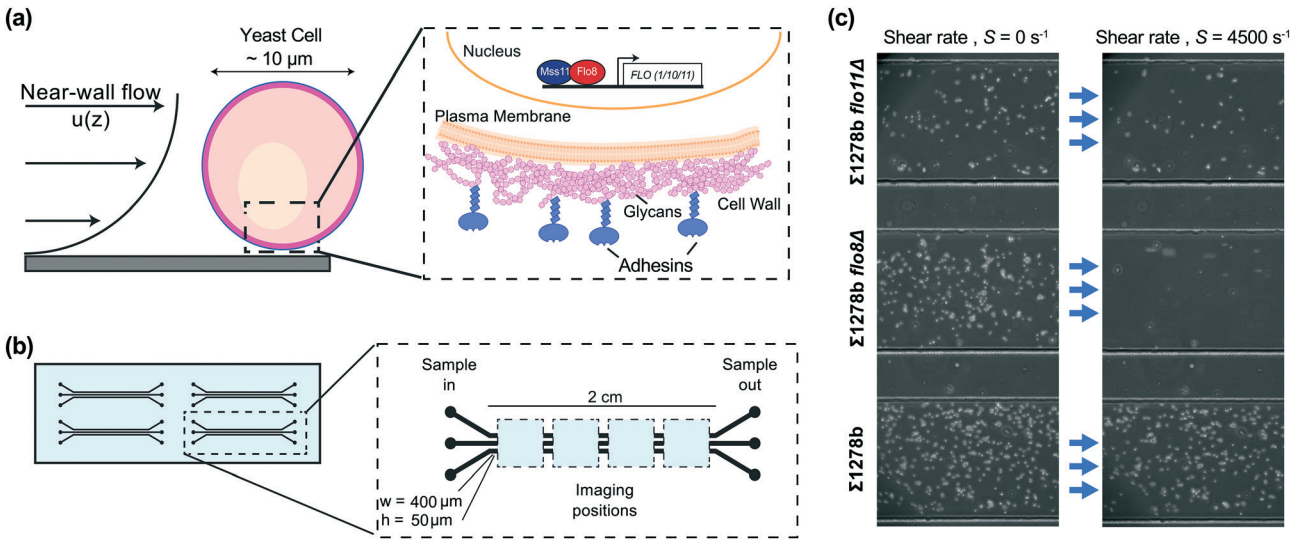

Fig. 1 Microfluidic assay for quantifying differential surface adhesion strength of yeast cells. (a) Schematic of a surface-adhered yeast cell exposed to hydrodynamic shear (left) and the components of the yeast cell wall including adhesin proteins, which participate in surface interactions (right). (b) Schematic of the microfluidic chip (left). Each chip has four devices consisting of three rectangular cross section microchannels for simultaneous acquisition of adhesion dynamics for three replicates or strains. Surface adhered cells are imaged at four positions along the channels (not drawn to scale) for sufficient statistics. (c) Example images of three *S. cerevisiae* strains in the absence of flow (left) and in the presence of flow (right), demonstrating differential adhesion strength of the yeast strains.

mechanics of yeast adhesion, including the re-localization of adhesin proteins in response to surface contact.[20–22] Such studies often rely on atomic force microscopy (AFM), which enables accurate quantification of attachment forces but is limited by extremely low throughput due to individual cell measurements. Fungal adhesive traits are known to be stochastic on an individual basis and can cause uncertainty in precision measurements of adhesion strength when considering a broad population of cells.[9,23,24] Hence, a need exists for assays which can provide population scale statistics on individual cell adhesion properties.

Here, we present a microfluidic assay (Fig. 1) for measuring surface adhesion properties of yeast strains, comprising customized microchannels and image analysis. The assay enables the direct quantification of the adhesive properties of three different yeast strains or replicates simultaneously by monitoring the adhesion state of thousands of cells per channel. Our approach is based on the application of precisely controlled hydrodynamic shear (Fig. 1a), which is proportional to the drag force on the cells (see ESI†) and systematically induces detachment from the surface (Fig. 1c). We demonstrate the efficacy of our assay by quantitatively comparing the differential adhesion of nine common *S. cerevisiae* laboratory strains and mutants lacking *FLO* family genes, which contribute to fungal adhesion. We show the distinct effects of ionic strength of the buffer solution and surface hydrophobicity on adhesion of the investigated yeast strains. Furthermore, we demonstrate how strain characteristics obtained from our assay can be applied for the separation and enrichment of cells with different adhesive properties – a feature of great potential for bioengineering applications.

2. Materials and methods

2.1 Growth and preparation of yeast suspensions

The *Saccharomyces cerevisiae* strains used in this work were: Σ1278b, Σ1278b *flo8Δ*, Σ1278b *flo11Δ*, W303-1A, SK1, SK1 *flo8Δ*, and EBY100 (see Table S1†).[25] For cell detachment assays, all strains were grown overnight in liquid YPD (yeast extract (1% w/v), peptone (2% w/v), dextrose (2% w/v)) medium at 30 °C with shaking, diluted into fresh media on the following day to OD_{600} = 0.2, and grown for 3 more hours or until OD_{600} = 1.0–1.5. A 1 mL volume of cell culture equivalent to OD_{600} = 3.0 was then washed twice with sterile water, once with 10 mM citric acid phosphate buffer pH 6.0 containing 150 mM, 75 mM, or 10 mM NaCl and resuspended in 3 mL of the same buffer at final concentration around 3×10^7 cells per mL. In yeast strain sorting experiments, cells were grown and washed as described above, resuspended in 10 mM citric acid phosphate buffer supplemented with 150 mM NaCl and mixed in desired proportions based on OD_{600} readings.

2.2 Device fabrication

Microfluidic devices used in the cell detachment assay consisted of three parallel rectangular channels (400 μm wide, 50 μm deep, and 2 cm long) for multiplexing measurements, with four devices per chip (Fig. 1b). The devices used in yeast strain sorting experiments had two parallel channels with dimensions of 400 μm in width, 70 μm in height and 5.5 cm in length, and were equipped with two inlet and two outlet openings (Fig. 5a). All devices were fabricated using standard soft-lithography techniques.[26] Briefly, a mold was prepared by spin coating photoresist (SU-82050, MicroChem Corp.) on a silicon wafer and patterning the devices through photolithography.

The microchannels were then cast in polydimethylsiloxane (PDMS, Dow Corning Corp.) and the devices were plasma-bonded to a standard glass microscope slide using hand-held plasma generator (BD-20AC Laboratory Corona Treater, ETP) for experiments shown on Fig. 1 through 4 or using a plasma cleaner (PE-25, Plasma Etch) for experiments shown on Fig. 5. For modified surface hydrophobicity, microchannels were bonded to a flat PDMS sheet[27] (see Fig. S4†).

2.3 Experimental setup

PDMS-on-glass channels were filled with 1 M NaOH, incubated for 20 minutes, and rinsed with 8 mL of water to produce a uniform hydrophilic surface.[28,29] Non-toxic polyethylene tubing was linked to the channels, which were connected to a syringe pump (Harvard Apparatus Inc.) with glass syringes (Hamilton™ Gastight™ Syringes) containing buffer and to syringes containing yeast cell suspensions through a three-way valve. The microchannels were first wetted by flowing buffer through the system at a flow rate of 100 μL min^{-1}. Next, 200 μL of yeast cell suspension was injected into the channels, and the cells were allowed to settle for 30 minutes, whereby attachment occurs spontaneously. For the cell detachment assay, the flow rate was exponentially increased in 14 steps from 1–1000 μl min^{-1}, corresponding to shear rates 110–108 550 s^{-1} (see ESI†) with each shear rate being held for 4 minutes in duration.

Yeast strain sorting experiments were performed as follows. NaOH-treated and washed microchannels were flushed with buffer, and the yeast cells were introduced through the cell suspension inlets as indicated on Fig. 5(a). The buffer outlet was kept closed during that procedure to avoid premature introduction of yeast cells into the collection tubing. Cells were allowed to settle for 30 minutes prior to flow initiation. First, a shear rate of 15 080 s^{-1} was applied for 4 minutes and the flow-through was collected into a sterile 50 mL tube prefilled with 10 mL of buffer. The outlet tubing was then removed from the first collection tube, the outside surface of the tubing was cleaned with 70% ethanol, and the tubing was then inserted into a new 50 mL collection tube prefilled with 10 mL buffer. Cells remaining on the channel surface at that point were collected by applying shear rate of 286 650 s^{-1} for 1 minute. Fractionation shear rates were informed by the relative detachment rates of each yeast strain (Fig. 5b). Cells were captured on the membrane of a sterile 0.2 μm polyether sulfone syringe filter (GE Healthcare Whatman™ Puradisc™ 25 mm filter) and collected by flushing the filter with 1 mL of sterile water to remove cells from the membrane. Eluate of the first fraction was diluted tenfold and 150 μl of resulting dilution was plated in triplicate on YPD agar plates. The eluate of the second fraction was plated directly on the YPD plates in triplicate by 150 μl for experiments shown on Fig. 5(c) or 1 mL of eluate was divided between 6 plates in experiments shown in Fig. 5(d) to plate all collected cells.

2.4 Image acquisition and analysis

For each applied shear rate, single images were captured at four different positions prior to flow initiation and three minutes after each increase in flow rate. Four positions were used to monitor a statistically significant number of cells in the microchannels, which provides greater accuracy in the evaluation of phenotypic diversity within cell population and increased statistical power of the collected data. The maximum Reynolds number in our assays was Re = 80, which suggests that the entrance length was $L = 0.06\ D_h\ Re = 1.9$ mm for the highest shear rate examined, where D_h is taken as the channel width. Therefore, the first position of imaging was chosen at a distance larger than 5 mm to eliminate any entrance effects. The three-minute timepoint was selected based on experiments showing that cell detachment reaches steady state within approximately 2.5 minutes following a step change in shear rate (Fig. S1 and ESI†). The syringe pump and image acquisition were automated (Nikon Elements) and imaging was performed on an inverted microscope (Nikon Ti-E, Nikon Instruments Inc.) using phase contrast (10×, 0.3 NA objective) and a sCMOS camera (Zyla 5.5, Andor Technology). Images of surface attached yeast cells were analysed using custom particle identification algorithms (MATLAB, MathWorks Inc.) incorporating background subtraction, intensity thresholding, and centroid detection.[30] Yeast cell detachment events were determined by comparing the number of cells on the microchannel surface following a step change in the shear rate at all four imaged positions. Monitoring cell detachment at multiple positions allows us to evaluate the uniformity of the results produced along the microchannels (see Fig. S2†). The number of cells on the surface at all four positions were then combined for appropriate representation of the examined cell populations and used to calculate fractions of cells on the channel surface. We thus report the fraction of cells remaining on the surface at a given shear rate as $f(S) = N(S)/N_{total}$, where $N(S)$ is the total number of attached cells at a given shear rate S, and N_{total} was typically in the range of $2–8 \times 10^3$ cells.

3. Results and discussion

3.1 Establishing microscale adhesion profiles of *S. cerevisiae* strains

We selected common laboratory yeast strains with known qualitative differences in adhesive properties, caused by a point mutation in the *FLO8* gene.[31] While qualitative differences of investigated yeast strains are readily observable (Fig. 1c), our microfluidic assay enables the precise quantitative comparison of various strains. To provide a comprehensive comparison of yeast surface adhesion strength across the different strains assayed, we calculated the detachment shear rates for all measured strains in several ways. First, by linearly interpolating the measured fraction of surface attached cells to $f(S) = 0.5$ to determine the median detachment shear rate S_m (Fig. S3 and Table S1†). The median detachment shear rate is a robust metric that enables the determination of the

adhesive strength over a broad range of cell adhesion phenotypes. However, the median detachment shear rate is difficult to measure for some weakly adhering cells exhibiting small $S_m < 100\ s^{-1}$, for example W303 (Fig. 2a). We found that the sigmoidal characteristics of the detachment curves are well fit by a Hill equation $f(S) = 1/(1 + (S/S_m)^n)$, where S_m is the median detachment shear rate, and n is the slope of the linear decay in log–log scale. Nonlinear regressions show excellent agreement ($R^2 > 0.99$) with the measured detachment curves (see Table S1†) and enable the extrapolation of S_m to small shear rates. Calculation of the mean value of the attachment survival probability from the measured $f(S)$ (Table S1†) as well as exponential fits (analysis not shown) showed qualitative agreement with the observed trends for S_m (see ESI†). Thus, from our microfluidic cell detachment assay, we report results in terms of the measured median detachment shear rate below and provide fitted detachment shear rates in Table S1.†

We first measured the detachment from glass surface of wildtype and *flo8* mutant diploid strains Σ1278b and W303, respectively (Fig. 2a). The fraction f of Σ1278b cells remaining on the substrate decreased slowly in a sigmoidal fashion with increasing shear rate S, while W303 cells lacking a functional *FLO8* gene were rapidly detached from the glass surface. For W303 cells, a fraction $f \approx 50\%$ remained attached to the surface at a shear rate $S_m \approx 100\ s^{-1}$. For comparison, the median detachment shear rate of W303 was over two orders of magnitude lower than for strain Σ1278b, which required a shear rate of $S_m \approx 27\,000\ s^{-1}$ to achieve $f \approx 50\%$ detachment (Fig. 2a).

The *FLO8* gene encodes a transcription factor responsible for activating the expression of yeast surface adhesins such as *FLO1*, *FLO10* and *FLO11*, and a glucoamylase gene *STA1*.[32,33] Flo1p adhesin has been shown to specifically bind to mannose molecules on the surface of neighbouring yeast cells and participates in flocculation.[5] In addition to flocculation, the surface adhesin Flo11p also mediates agar invasion and adhesion to polystyrene.[34–36] To determine whether ploidy affects adhesion, we measured the detachment shear rate of haploid Σ1278b (1n) and W303 (1n) cells in comparison to their diploid counterparts (Fig. 2a). The surface detachment profiles of Σ1278b (1n) and W303 (1n) strains were nearly identical to those of the diploid cells, suggesting that adhesion to an abiotic surface like glass is mediated by yeast cell wall components independent of ploidy.

3.2 Quantification of yeast strain-specific differences in adhesion

If the observed differences in adhesion strength between Σ1278b and W303 strains were indeed due to the mutation of *FLO8* gene in W303, then deletion of *FLO8* in a strongly adhesive strain, such as Σ1278b, should reduce its adhesive properties. To test this hypothesis, we measured the adhesive strength of Σ1278b *flo8Δ* cells using our microfluidic assay. The detachment shear rate in this strain ($S_m < 100\ s^{-1}$; Fig. 2b) was reduced by over two orders of magnitude relative to the parental strain. As expected, Σ1278b *flo8Δ* cells

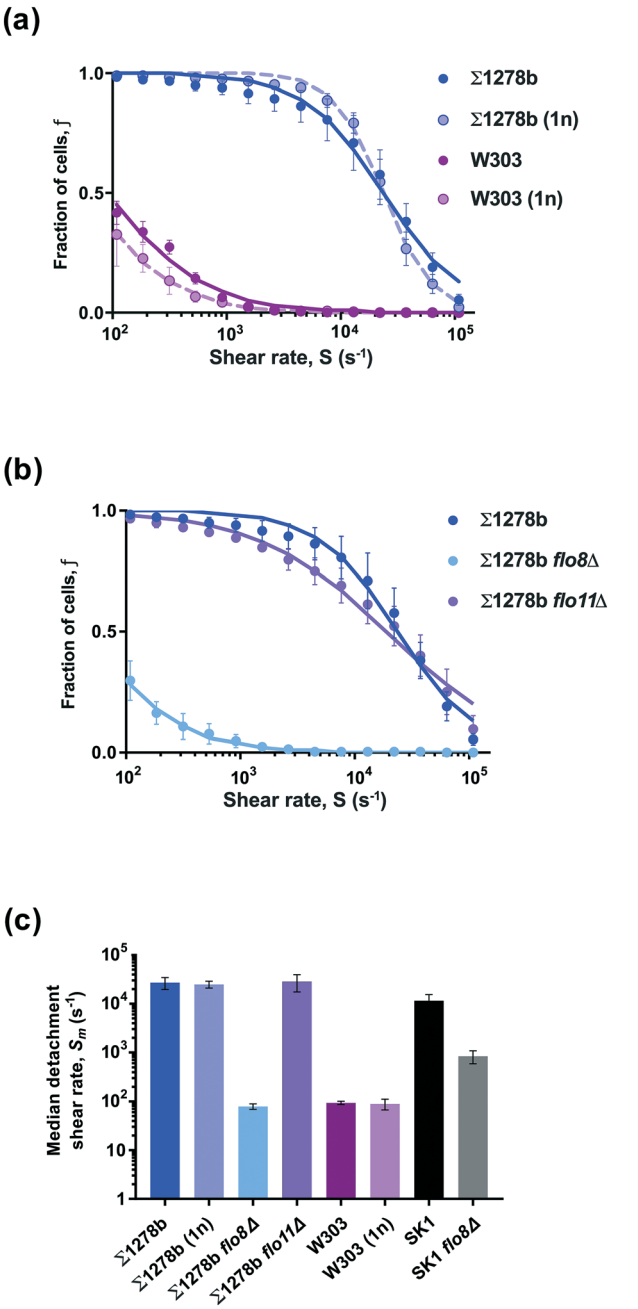

Fig. 2 Differential adhesion strength in *S. cerevisiae* strains is due to variations in genetic background. (a and b) Starting from no shear, the fraction of surface attached cells remaining on the microchannel surface (glass) is measured as a function of the applied shear rate. Data points show detected cells on the surface, error bars are standard error of the mean (SEM, $n = 3$), and curves are fits of the Hill equation to the data (fitted slopes shown in Table S1†). (a) Strains Σ1278b and W303 (diploid, 2n) show strongly differential adhesion. However, haploid (1n) strains of the same genetic background show comparable detachment rates to their diploid counterparts. (b) Strong adhesion of strain Σ1278b is not affected by the deletion of a single surface protein Flo11p in Σ1278b *flo11Δ* but is diminished by the deletion of *FLO8* gene in Σ1278b *flo8Δ* mutant. (c) Characteristic adhesive strength for each strain is quantified by the median detachment shear rate S_m for the cell population, which varies over two orders of magnitude. Error bars are SEM ($n = 3$).

performed similarly to *FLO8* deficient strain W303 in our adhesion assay and were released from surface at lower applied shear rates compared to wild-type Σ1278b cells. To evaluate if the strong adhesion of Σ1278b is mediated by Flo8-dependent adhesin Flo11p, we measured the detachment rate of Σ1278b *flo11Δ* cells and observed virtually no difference in the detachment profile compared to wild-type Σ1278b strain (Fig. 2b and c). This indicates that adhesion of Σ1278b cells to a glass surface is not mediated by Flo11p under tested conditions. To confirm the importance of the *FLO8* gene, we tested a second strongly adherent strain, SK1,[37] and its *FLO8* deletion carrying mutant SK1 *flo8Δ* (Fig. 2c). The *flo8* deletion reduced the attachment strength of SK1 from $S_m \approx 10\,000\ s^{-1}$ to $<1000\ s^{-1}$. While the attachment strength decreased about ten-fold, interestingly, the effect was not as drastic for the SK1 strain as compared to Σ1278b. These results suggest that Flo8 driven expression of yeast surface adhesins is not the sole mechanism of yeast adhesion to abiotic surfaces, and related *S. cerevisiae* strains may differ significantly in cell wall surface properties.

3.3 Electrostatic effects on yeast adhesion

Cell surface properties, such as hydrophobicity and surface charge, have been shown to vary significantly among industrial and laboratory yeast strains.[38] Non-specific cell adhesion to a surface depends upon the balance of van der Waals attractive forces and attractive or repulsive electrostatic interactions, which are influenced by the ionic strength of the culture medium through charge screening.[39,40] To determine the effect of ionic strength on yeast adhesion, we measured the median detachment shear rate of Σ1278b cells on a glass surface at NaCl concentration of 75 mM, and 10 mM, in addition to the concentration of 150 mM (Fig. 3). At low ionic strength, the median detachment shear rate of Σ1278b cells decreased significantly from $S_m \approx 27\,000\ s^{-1}$ at [NaCl] = 150 mM to $S_m \approx 1000\ s^{-1}$ at [NaCl] = 10 mM. This effect was not observed for W303 and Σ1278b *flo8Δ*, which lack a functional *FLO8* gene. Moreover, to confirm that differences in adherence seen at different NaCl concentrations are not due to osmosis-driven changes in yeast cell volume, we measured cell size in 10 mM, 75 mM, and 150 mM NaCl over the course of 2 hours and observed no significant deviation from normal size variation (Fig. S5†). The cell surface of yeast is heavily modified with sugars and negatively charged[41] at pH 6.0. Thus, this result is consistent with the theory that at low ionic strength, cell adhesion may be inhibited by electrostatic repulsion between the negatively-charged cell surface and the negatively-charged glass.

3.4 Effects of surface properties on yeast adhesion

The expression of *FLO1* and *FLO11* genes in yeast is known to increase cell surface hydrophobicity in industrial *S. cerevisiae* strains, which is in concordance with observed Flo11-mediated adhesion to plastics.[36,42] The expression of both *FLO1* and *FLO11* genes is controlled by the Flo8 transcription factor, suggesting that *FLO8* wild-type and mutant cells may exhibit differential adhesion strength to hydrophobic *versus* hydrophilic surfaces. In order to test the effect of substrate hydrophobicity on yeast adhesion, microfluidic devices were bonded to a flat sheet of PDMS, which is known to be hydrophobic (contact angle $\theta_c > 100°$; Fig. S4†),[38,43] to compare

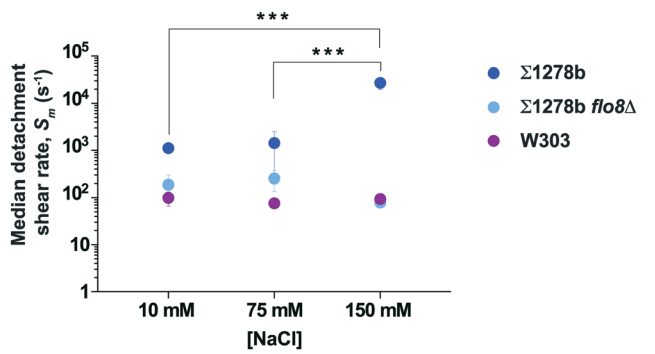

Fig. 3 Ionic strength affects yeast adhesion to surfaces. Median detachment shear rates S_m of Σ1278b, Σ1278b *flo8Δ* and W303 strains at three different sodium chloride concentrations ([NaCl] = 10, 75, and 150 mM). Σ1278b shows a strong NaCl-concentration dependent increase of the median detachment shear rate, while Σ1278b *flo8Δ* and W303 strains display no salt concentration dependence in adhesion to glass. Error bars are SEM (n = 3), and the asterisks (***) indicate significant difference based on a two-way ANOVA test, $p < 0.0005$.

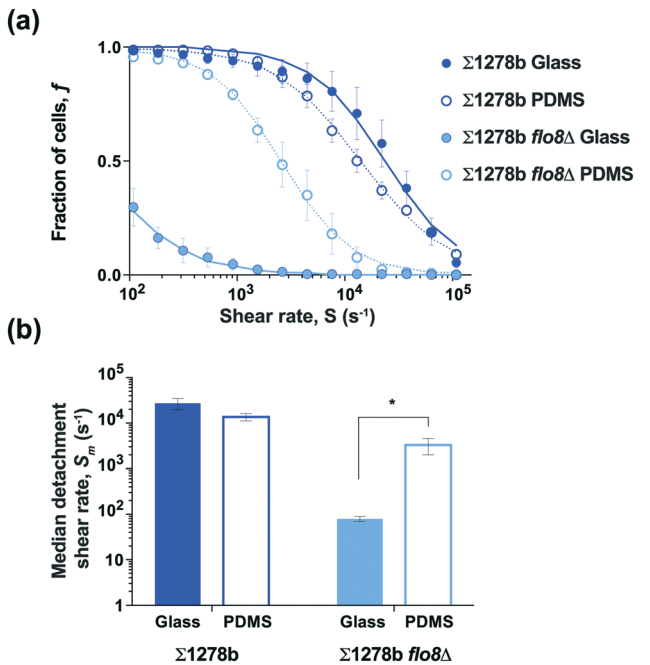

Fig. 4 Surface hydrophobicity of glass and PDMS differentially affect yeast adhesion. (a) The fractions of remaining surface attached yeast strains Σ1278b and Σ1278b *flo8Δ* on glass and PDMS substrates over a range of increasing shear rates. Sodium chloride buffer concentration was fixed at [NaCl] = 150 mM. (b) Median detachment shear rates for the strains shown in (a). Error bars are SEM (n = 3), and the asterisk (*) indicates significant difference based on a Student's t-test, p = 0.06.

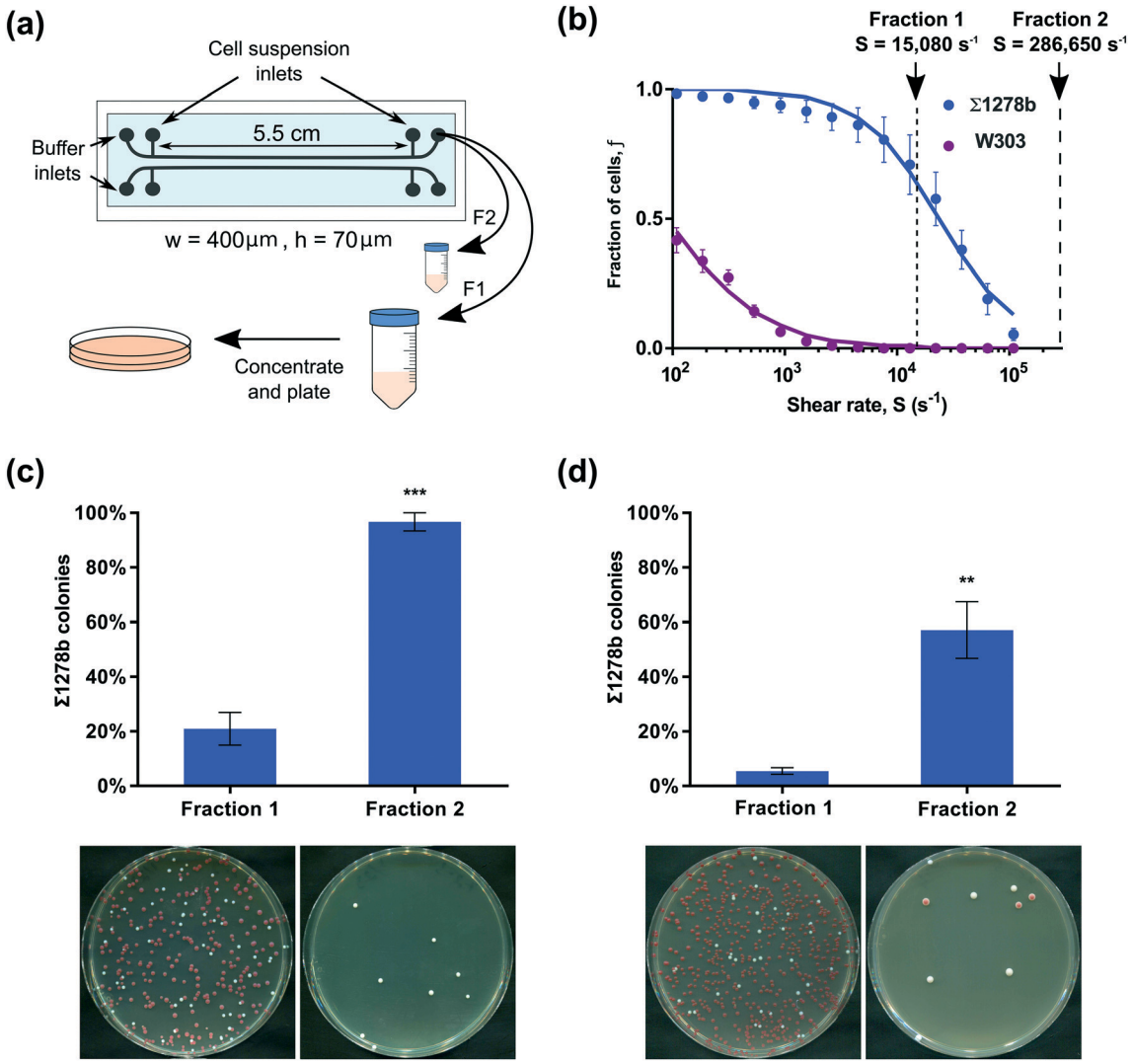

Fig. 5 Microfluidic separation of yeast cells based on surface adhesive properties. (a) Schematic of experimental design and microchannels used in yeast strain sorting experiments. (b) Separation was achieved using a shear rate S = 15 080 s^{-1}, and remaining fraction of cells was removed using S = 286 650 s^{-1}. (c) Percent of Σ1278b colonies in two collected fractions from sorting experiments with initial W303 to Σ1278b concentration ratio 3 : 2. Asterisks (***) indicate p-value of p = 0.0004 based on Student's t-test. Photos under each bar demonstrate representative plates used to count colonies – white colonies are Σ1278b, red colonies are W303. (d) Percent of Σ1278b colonies in two collected fractions from cell suspension with initial W303 to Σ1278b ratio 14 : 1. Asterisks (**) indicate p-value of p = 0.0077 based on Student's t-test.

with the hydrophilic glass substrate used above (contact angle $\theta_c \approx 10°$; Fig. 1–3 and S4†). The wild-type strain Σ1278b showed no significant difference in the median detachment shear rate between the glass and PDMS substrates (Fig. 4). Surprisingly, the median detachment shear rate of Σ1278b *flo8Δ* strain increased dramatically from S_m = 80 s^{-1} to ≈ 3000 s^{-1}, when assayed on a hydrophobic PDMS surface (Fig. 4 and Table S1†). These results suggest that in the absence of electrostatic repulsive forces, even cells lacking major surface adhesins retain affinity for a more hydrophobic surface.

3.5 Separation of yeast cells based on adhesive properties

Emergent yeast surface display techniques show great promise for the development of antibodies and small peptide therapeutics.[25] Such approaches exploit sequential rounds of expression of protein libraries on yeast surfaces, selection of cells to recognize soluble or solid-phase conjugated targets, and collection and regrowth of selected clones.[44,45] The microfluidic yeast cell screening techniques demonstrated here, have great potential for yeast display and bioengineering applications to perform clone selection on surface-conjugated targets. To demonstrate the potential of our assay to separate yeast strains based on surface attachment strength, we performed a series of sorting experiments to fractionate strongly adherent yeast from weakly adherent cells.

Two yeast strains displaying differential median detachment shear rates (W303 and Σ1278b, see Fig. 2a) were combined to form an artificially mixed cell population, and then fractionated using our microfluidic assay. The W303 strain

carries a mutation in *ADE2*, resulting in the accumulation of a coloured intermediate. Consequently, W303 colonies grown on agar plates in aerobic conditions gradually turn red allowing them to be easily distinguished from white-coloured Σ1278b colonies and to determine the efficacy of the yeast cell separation. W303 and Σ1278b cells were combined in a 3 : 2 ratio, respectively, and allowed to attach to the channel surface (Fig. 5a). A shear rate of 15 080 s^{-1} was applied for four minutes to remove the bulk of the weakly attached W303 cells. Based on detachment profiles measured in our microfluidic adhesion assay and confirmed in single shear rate experiments (see ESI† and Fig. S6), up to 70% of strain Σ1278b cells from the mixed population were expected to remain surface attached up to this shear rate (Fig. 5b). The detached fraction of cells was captured in a sterile collection tube. Subsequently, the remaining fraction of surface attached cells – comprising mostly Σ1278b – was then collected by applying a shear rate of 286 650 s^{-1}, which is well beyond the Σ1278b median detachment rate for 1 minute (Fig. 5a and b). Notably, we have confirmed that such a high shear rate (286 650 s^{-1}) used to collect the second fraction has no deleterious effects on yeast cells (Fig. S7†). To evaluate strain composition of the two collected fractions, both cell suspensions were concentrated and plated on YPD agar plates. As predicted based on the measurements in our adhesion assay, 96% of cells in the strongly-attached fraction were Σ1278b, while only 4% were W303, showing that characteristics obtained above can be used to sort cells based on adherence (Fig. 5c). We speculate that the presence of W303 cells in the strongly-adherent fraction could be explained in two possible ways – first, W303 and Σ1278b could be attaching to each other, causing the less adherent W303 cells to withstand high shear rates relying on Σ1278b strain's adherence to glass. Second, the adhesion assay is performed by gradually increasing shear rates over time while strain separation was done by applying a single shear rate and ultimately reducing the period of time over which the cells were sheared. Although we did not observe cell detachment after four minutes of constant shear in preliminary experiments (Fig. S1†), it is possible that increasing shear rate over longer periods of time may facilitate cell detachment.

To evaluate the robustness of this method, we tested our approach by reducing the number of Σ1278b cells in the sorting experiment and changed the W303 to Σ1278b ratio to 14 : 1, respectively. Only 5% of observed colonies from fraction 1 were Σ1278b, while 57% of the second fraction were Σ1278b (Fig. 5d). Taking into account the small concentration of Σ1278b cells in the initial suspension, the observed ratio of Σ1278b in the second fraction further emphasises the utility of the strain characteristics obtained earlier for screening and selection processes. Based on these observations, the selected fraction could be further enriched through additional rounds of fractionation to isolate Σ1278b cells from the total population. Furthermore, we have been able to successfully collect fractions of weakly adherent W303 cells from a mixture of W303 and Σ1278b, albeit with slightly lower efficiency after the first round of fractionation (see ESI† and Fig. S8), using the present approach. Taken together, we demonstrated that surface adhesion traits quantified through our assay can be used to select the optimal shear rates for cell separation based on adhesive properties.

Conclusions

In this work, we developed and validated the efficacy of a microfluidic assay for quantifying yeast surface adhesion strength *via* the precise control of hydrodynamic shear and image analysis. The resolution of the step-wise increase of shear rate in this assay can be arbitrarily adjusted to capture a wide range of adhesive strengths across a variety of yeast strains. We demonstrated that our assay enables the detection of differences in adhesion based on genetic background; the *FLO8* gene deletion decreases adhesive strength to a varying degree in Σ1278b and SK1 strains. This methodology was applied to determine effects of environmental conditions and surface composition on yeast adhesive strength. Furthermore, by capturing the cells detaching at specific shear rates, we demonstrated the ability of our assay to separate cells with differential surface adhesion strength from a mixed cell population. Specifically, combining our assay with an outgrowth phase or multi-stage microfluidic separation would lead to separation of cells from mixtures of more than two strains if differences in adherence exist. Such approaches can be applied even when the detachment profiles of cells under investigation are not known, as fractionation can be performed based on adhesive properties prior to exact identification of strains in the studied mixture of cells.

The median detachment shear rate S_m provides a concrete metric for discerning adhesive strength of cells and can be calibrated for direct force measurements to complement techniques such as AFM. Fungal adhesion is of great concern to both medical and industrial communities, and thus, this approach will have utility in future applications for determining genetic and environmental factors that contribute to surface adhesion in many fungal species. For example, the quantification of pathogenic yeast interactions with hydrophilic and hydrophobic surfaces will aid in testing of anti-fungal compounds and the development of materials used in medical implants.[46] Other potential applications include quantitative evaluation of yeast adhesion on a population level for fitness heterogeneity and biofilm studies as well as establishing baseline detachment shear rate of strains used for protein engineering. Display of protein libraries on yeast surface has been widely adapted for antibody and biologics development and screening. Most often, magnetic beads are used as solid carriers of antigens, however, silicon surfaces are amenable to functionalization and subsequent conjugation of peptides and nucleic acids. Our microfluidic assay coupled with antigen-coated channels could be used to determine yeast background adhesion, counterselection, and selection of yeast clones with differential affinity to the target.

Author contributions

K. R. and A. D. performed the experiments and analysed the data. K. R. was responsible for all cell manipulations and

imaging and A. D. designed the microfluidic devices, developed microscope automation protocols, and image analysis software. All authors conceived and designed the experiments and wrote and edited the manuscript.

Conflicts of interest

There are no conflicts to declare.

Acknowledgements

This work was funded in part by Army Research Office Grant W911NF-16-1-0175 (to S. M. F.) and by National Science Foundation Grants CAREER-1554095 and CBET-1511340 (to J. S. G.). This work was also supported by at Tufts Collaborates grant (to S. M. F. and J. S. G.).

References

1 K. J. Verstrepen and F. M. Klis, *Mol. Microbiol.*, 2006, **60**, 5–15.
2 J. R. Blankenship and A. P. Mitchell, *Curr. Opin. Microbiol.*, 2006, **9**, 588–594.
3 S. E. Van Mulders, M. Ghequire, L. Daenen, P. J. Verbelen, K. J. Verstrepen and F. R. Delvaux, *Appl. Microbiol. Biotechnol.*, 2010, **88**, 1321–1331.
4 O. Kobayashi, N. Hayashi, R. Kuroki and H. Sone, *J. Bacteriol.*, 1998, **180**, 6503–6510.
5 K. V. Goossens, C. Stassen, I. Stals, D. S. Donohue, B. Devreese, H. De Greve and R. G. Willaert, *Eukaryotic Cell*, 2011, **10**, 110–117.
6 M. L. Zupancic, M. Frieman, D. Smith, R. A. Alvarez, R. D. Cummings and B. P. Cormack, *Mol. Microbiol.*, 2008, **68**, 547–559.
7 D. J. Rigden, L. V. Mello and M. Y. Galperin, *Trends Biochem. Sci.*, 2004, **29**, 335–339.
8 X. Xie and P. N. Lipke, *Yeast*, 2010, **27**, 479–488.
9 M. Fidalgo, R. R. Barrales and J. Jimenez, *Yeast*, 2008, **25**, 879–889.
10 J. Chandra, P. K. Mukherjee, S. D. Leidich, F. F. Faddoul, L. L. Hoyer, L. J. Douglas and M. A. Ghannoum, *J. Dent. Res.*, 2001, **80**, 903–908.
11 S. Smukalla, M. Caldara, N. Pochet, A. Beauvais, S. Guadagnini, C. Yan, M. D. Vinces, A. Jansen, M. C. Prevost, J. P. Latge, G. R. Fink, K. R. Foster and K. J. Verstrepen, *Cell*, 2008, **135**, 726–737.
12 V. Nedovic, B. Gibson, T. F. Mantzouridou, B. Bugarski, V. Djordjevic, A. Kalusevic, A. Paraskevopoulou, M. Sandell, D. Smogrovicova and M. Yilmaztekin, *Yeast*, 2015, **32**, 173–216.
13 J. Wu, A. Elliston, G. Le Gall, I. J. Colquhoun, S. R. A. Collins, J. Dicks, I. N. Roberts and K. W. Waldron, *Sci. Rep.*, 2017, **7**, 14259.
14 G. A. O'Toole, L. A. Pratt, P. I. Watnick, D. K. Newman, V. B. Weaver and R. Kolter, *Methods Enzymol.*, 1999, **310**, 91–109.
15 H. C. Flemming and J. Wingender, *Nat. Rev. Microbiol.*, 2010, **8**, 623–633.
16 M. H. Meem and P. J. Cullen, *FEMS Yeast Res.*, 2012, **12**, 809–818.
17 B. Guo, C. A. Styles, Q. Feng and G. R. Fink, *Proc. Natl. Acad. Sci. U. S. A.*, 2000, **97**, 12158–12163.
18 W. Kueng, E. Silber and U. Eppenberger, *Anal. Biochem.*, 1989, **182**, 16–19.
19 S. Bruckner and H. U. Mosch, *FEMS Microbiol. Rev.*, 2012, **36**, 25–58.
20 C. X. Chan, S. El-Kirat-Chatel, I. G. Joseph, D. N. Jackson, C. B. Ramsook, Y. F. Dufrene and P. N. Lipke, *mSphere*, 2016, **1**, e00128-16.
21 D. Alsteens, M. C. Garcia, P. N. Lipke and Y. F. Dufrene, *Proc. Natl. Acad. Sci. U. S. A.*, 2010, **107**, 20744–20749.
22 P. N. Lipke, S. A. Klotz, Y. F. Dufrene, D. N. Jackson and M. C. Garcia-Sherman, *Microbiol. Mol. Biol. Rev.*, 2018, **82**, e00035-17.
23 B. L. Chin, O. Ryan, F. Lewitter, C. Boone and G. R. Fink, *Genetics*, 2012, **192**, 1523–1532.
24 K. J. Verstrepen, T. B. Reynolds and G. R. Fink, *Nat. Rev. Microbiol.*, 2004, **2**, 533–540.
25 E. T. Boder and K. D. Wittrup, *Nat. Biotechnol.*, 1997, **15**, 553–557.
26 Y. Xia and G. M. Whitesides, *Annu. Rev. Mater. Sci.*, 1998, **28**, 153–184.
27 K. Haubert, T. Drier and D. Beebe, *Lab Chip*, 2006, **6**, 1548–1549.
28 I. Hoek, F. Tho and W. M. Arnold, *Lab Chip*, 2010, **10**, 2283–2285.
29 J. J. Cras, C. A. Rowe-Taitt, D. A. Nivens and F. S. Ligler, *Biosens. Bioelectron.*, 1999, **14**, 683–688.
30 J. C. Crocker and D. G. Grier, *J. Colloid Interface Sci.*, 1996, **179**, 298–310.
31 H. Liu, C. A. Styles and G. R. Fink, *Genetics*, 1996, **144**, 967–978.
32 O. Kobayashi, H. Suda, T. Ohtani and H. Sone, *Mol. Gen. Genet.*, 1996, **251**, 707–715.
33 O. Kobayashi, H. Yoshimoto and H. Sone, *Curr. Genet.*, 1999, **36**, 256–261.
34 W. S. Lo and A. M. Dranginis, *Mol. Biol. Cell*, 1998, **9**, 161–171.
35 K. V. Goossens and R. G. Willaert, *FEMS Yeast Res.*, 2012, **12**, 78–87.
36 F. Li and S. P. Palecek, *Eukaryotic Cell*, 2003, **2**, 1266–1273.
37 K. Nowlin, A. Boseman, A. Covell and D. LaJeunesse, *J. R. Soc., Interface*, 2015, **12**, 20140999.
38 M. Schiavone, S. Dejean, N. Sieczkowski, M. Castex, E. Dague and J. M. Francois, *Front. Microbiol.*, 2017, **8**, 1806.
39 M. Hermanssonm, *Colloids Surf., B*, 1999, **14**, 105–119.
40 D. Kregiel, J. Berlowska and W. Ambroziak, *World J. Microbiol. Biotechnol.*, 2012, **28**, 3399–3408.
41 P. Thonart, M. Custinne and M. Paquot, *Enzyme Microb. Technol.*, 1982, **4**, 191–194.
42 P. Govender, J. L. Domingo, M. C. Bester, I. S. Pretorius and F. F. Bauer, *Appl. Environ. Microbiol.*, 2008, **74**, 6041–6052.

43 A. Mata, A. J. Fleischman and S. Roy, *Biomed. Microdevices*, 2005, **7**, 281–293.
44 H. R. Hoogenboom, *Nat. Biotechnol.*, 2005, **23**, 1105–1116.
45 J. A. Van Deventer and K. D. Wittrup, *Methods Mol. Biol.*, 2014, **1131**, 151–181.
46 M. Ramasamy and J. Lee, *BioMed Res. Int.*, 2016, **2016**, 1851242.